

Efficient Host–Guest Energy Transfer in Polycationic Cyclophane–Perylene Diimide Complexes in Water

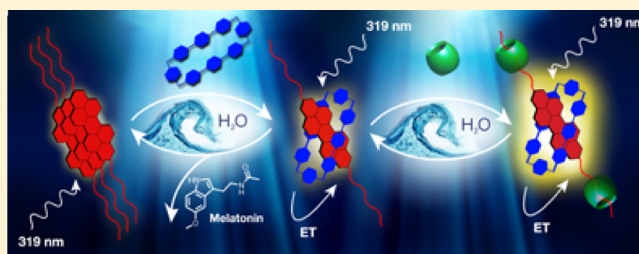
Seán T. J. Ryan,[†] Jesús Del Barrio,[†] Indrajit Ghosh,[‡] Frank Biedermann,[‡] Alexandra I. Lazar,[‡] Yang Lan,[†] Roger J. Coulston,[†] Werner M. Nau,^{*,‡} and Oren A. Scherman^{*,†}

[†]Melville Laboratory for Polymer Synthesis, Department of Chemistry, University of Cambridge, Lensfield Road, Cambridge CB2 1EW, United Kingdom

[‡]School of Engineering and Science, Jacobs University Bremen, Campus Ring 1, 28759 Bremen, Germany

S Supporting Information

ABSTRACT: We report the self-assembly of a series of highly charged supramolecular complexes in aqueous media composed of cyclobis(4,4'-(1,4-phenylene)bispiperidine-*p*-phenylene)tetrakis(chloride) (ExBox) and three dicationic perylene diimides (PDIs). Efficient energy transfer (ET) is observed between the host and guests. Additionally, we show that our hexacationic complexes are capable of further complexation with neutral cucurbit[7]uril (CB[7]), producing a 3-polypseudorotaxane via the self-assembly of orthogonal recognition moieties. ExBox serves as the central ring, complexing to the PDI core, while two CB[7]s behave as supramolecular stoppers, binding to the two outer quaternary ammonium motifs. The formation of the 3-polypseudorotaxane results in far superior photophysical properties of the central PDI unit relative to the binary complexes at stoichiometric ratios. Lastly, we also demonstrate the ability of our binary complexes to act as a highly selective chemosensing ensemble for the neurotransmitter melatonin.



INTRODUCTION

A major goal of supramolecular chemistry is to achieve a greater understanding of nature through synthetic mimicking of biological structures and processes in the laboratory.¹ To this end, a significant amount of research has been conducted into supramolecular recognition motifs and their assembly into functional constructs. Most of this research has been conducted in organic media, which offer advantages of solubility and a lower degree of solvent interference when compared to aqueous media.² However, the role of water in complex biological processes is ubiquitous. Therefore, it is of great importance to investigate new, synthetic water-mediated assemblies, which efficiently mimic important biological processes.³

Energy transfer (ET) is one such process that is essential for the existence of the majority of life on earth on account of its role in the photosynthetic pathway.⁴ Much attention has been afforded to covalently linked systems capable of *biomimicking* this phenomenon as they offer potential in new light-harvesting devices for which molecular wires, photon harvesting polymers and dendrimers have received particular interest.⁵ Self-assembly offers an attractive, complementary route to realizing systems capable of undergoing efficient energy transfer as it replaces arduous synthesis with simple mixing of recognition units in solution. It also allows for the controlled, reversible assembly of components leading to sensory materials.⁶ Supramolecular ET sensors have demonstrated great potential for numerous applications including high-throughput screens of biologically

relevant analytes, real-time monitoring of cellular glucose flux and gene discovery.⁷ Supramolecular ET sensors may be realized by a variety of different methods and allow for tailored design and optimization with high signal-to-noise ratios.⁸ Examples of supramolecular host–guest complexation to achieve systems that undergo ET, however, are rare in the literature, most of which use organic solvents to mediate self-assembly.⁹ Derivatized cyclodextrins have received attention for the assembly of chromophores in water.¹⁰ In these examples, the hydrophobic cavity of the cyclodextrin acts as the recognition unit for dye complexation.

Herein, we report the first water-mediated assembly of a series of binary host–guest complexes capable of undergoing efficient ET, where the chromophores themselves act as the recognition units. The complexes represent a new ET pair and are composed of the recently reported tetracationic cyclophane, cyclobis(4,4'-(1,4-phenylene)bispiperidine-*p*-phenylene)tetrakis(chloride) (ExBox) (donor),¹¹ and a series of dicationic perylene diimides (PDIs) (acceptors) as shown in Figure 1, panels a and b, respectively. The direct recognition of the ET pairs allows for very small spatial separation between the chromophores leading to efficient ET. Furthermore, the hexacationic character of these complexes exemplifies the power of the hydrophobic effect to drive self-assembly despite substantial Coulombic repulsion.¹²

Received: April 1, 2014

Published: June 3, 2014

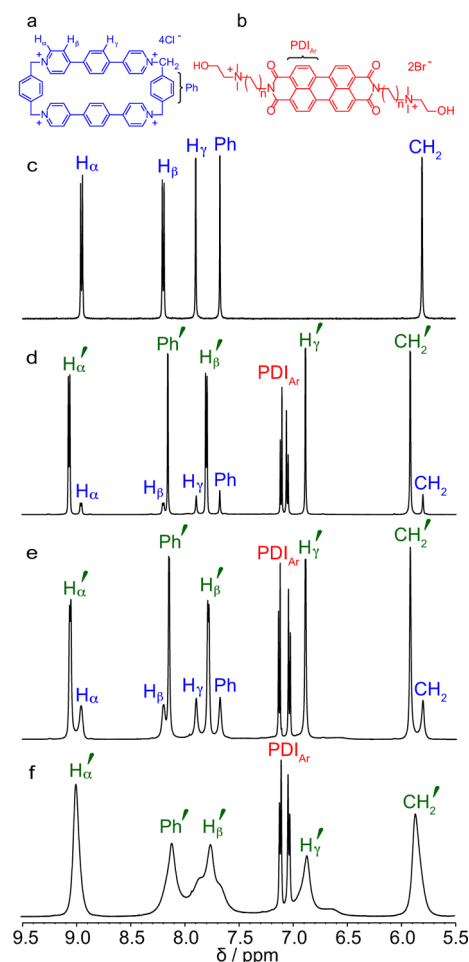


Figure 1. Chemical structures of (a) ExBox (donor) and (b) the PDIs (acceptors) used in this study ($n = 1$ for **PDI-E**, $n = 2$ for **PDI-B**, $n = 3$ for **PDI-H**). ^1H NMR spectra of the aromatic regions of (c) ExBox, (d) **PDI-E**:ExBox 1:1, (e) **PDI-B**:ExBox 1:1, and (f) **PDI-H**:ExBox 1:1 (D_2O , 3 mM). Primes indicate complexed peaks.

Tetracationic cyclophanes and their incorporation into functional nanoassemblies have been studied extensively since the late 1980s.¹³ Recently, interest in a new series of extended variants of the classic cyclophane receptor, “Blue Box”, the ExⁿBox series, has developed, of which ExBox is also designated Ex¹Box.^{11,14} The extended cavities of the ExⁿBox series allow for novel modes of binding of small aromatic guests as well as the complexation of large, π -electron-rich guests. Such ability has led to claims that these materials could find use in new photodriven systems and light-harvesting applications.¹⁵ PDIs have also been investigated for their exceptional electronic properties and light-harvesting abilities.¹⁶

RESULTS AND DISCUSSION

The interaction between ExBox and a series of symmetrically substituted, diatonic perylene diimides (**PDI-E**, **PDI-B**, and **PDI-H**, Figure 1a,b) was studied by a full range of one- and two-dimensional NMR techniques. ^1H NMR titrations (Figures 1c–f and S1–S3) of the PDIs into ExBox in D_2O reveal downfield shifts of ExBox protons H_α , Ph and CH_2 and strong upfield shifts of H_γ and H_β . This shifting behavior is in excellent agreement to that previously observed for the binding of polycyclic aromatic hydrocarbons (PAHs) to ExBox- PF_6 in acetonitrile.¹¹ The PDI_{Ar} protons also show good resolution

demonstrating the disruption of the PDI π -stacks in water via cavity complexation.¹⁷ However, in contrast to the binding with PAHs, the presence of complexed and uncomplexed ExBox peaks show that these complexes undergo slow exchange on the NMR time scale. This is presumably due to an electrostatic barrier to threading and dethreading caused by the two positively charged quaternary ammonium groups of the dicationic PDIs.¹⁸ The absence of uncomplexed PDI_{Ar} peaks is due to aggregation of the free PDI, which heavily suppresses these signals as previously documented.¹⁷ The spectra also show a trend whereby the propensity of the PDIs to stack in water increases with an increase in tether length (the length between the imide nitrogen atoms and the quaternary ammonium motifs), evidenced by an increased broadening of complexed and uncomplexed ExBox peaks (Figures 1 and S4). The increase in stacking propensity with tether length is expected since more distal cationic groups cause lower intermolecular electrostatic repulsion. This was independently verified through a decrease in fluorescence quantum yield of the PDI dyes with longer tethers (Table 1), since the detected

Table 1. Photophysical Properties of the PDI Dyes in the Absence and Presence of ExBox

guest (acceptor)	host (donor)	quantum yield (Φ_f) ^a	PDI lifetime (τ_f , ns) ^b
PDI-E		0.06 ± 0.01^c	4.61
	ExBox	0.36^d	6.3
	CB[8]	0.62	5.9^e
PDI-B		0.018	4.41
	ExBox	0.36^d	6.2
	ExBox + 2CB[7]	0.47	7.11
PDI-H		0.008	4.83
	ExBox	0.36^d	6.2

^aDetermined by relative measurement using a $15 \mu\text{M}$ solution of **PDI-E** in water as standard (first entry of this table). ^bDetermined by TCSPC $\lambda_{\text{ex}} = 500 \text{ nm}$, $\lambda_{\text{mon}} = 550 \text{ nm}$ (statistical error $\pm 3\%$) at $50 \mu\text{M}$ guest and large excess of host. ^cValue determined for a $15 \mu\text{M}$ solution with Rhodamine 6G in ethanol as quantum yield standard ($\phi = 0.95$); value for a $1.5 \mu\text{M}$ solution: 0.28 ± 0.03 ; value previously determined with a $10 \mu\text{M}$ solution with fluorescein as standard: 0.03 .¹⁷ ^dDetermined upon saturation of PDIs with ExBox. ^eFrom ref 17.

emission is assigned to (unstacked) monomer emission. Two-dimensional DOSY NMR also confirmed binding as the PDI_{Ar} peaks align with those corresponding to complexed ExBox, demonstrating that the two species diffuse at equal rates (Figure S5). Two more species are observed in the DOSY spectra: the uncomplexed ExBox and PDI aggregates, which diffuse at faster and slower rates, respectively, indicative of their lower and higher molecular masses. Through-space ROESY NMR (Figure S6) shows correlation between the PDI_{Ar} peaks and the H_α , H_β and Ph protons of ExBox, demonstrating the small spatial separation (ca. 3.5 \AA)¹¹ between the chromophores.

With the formation of host–guest complexes between ExBox and the PDIs firmly established by NMR, we proceeded to the photophysical characterization. First, the formation of the host–guest complexes was followed by optical titrations, which induced a narrowing of the PDI UV/vis spectra upon addition of ExBox, with an increase in optical density near 520–550 nm (Figure S7). More significantly, a 2.1-, 6.3-, and 12.6-fold increase in fluorescence of **PDI-E**, **PDI-B**, and **PDI-H** ($15 \mu\text{M}$) upon addition of ExBox ($15 \mu\text{M}$) was observed (Figures 2d and

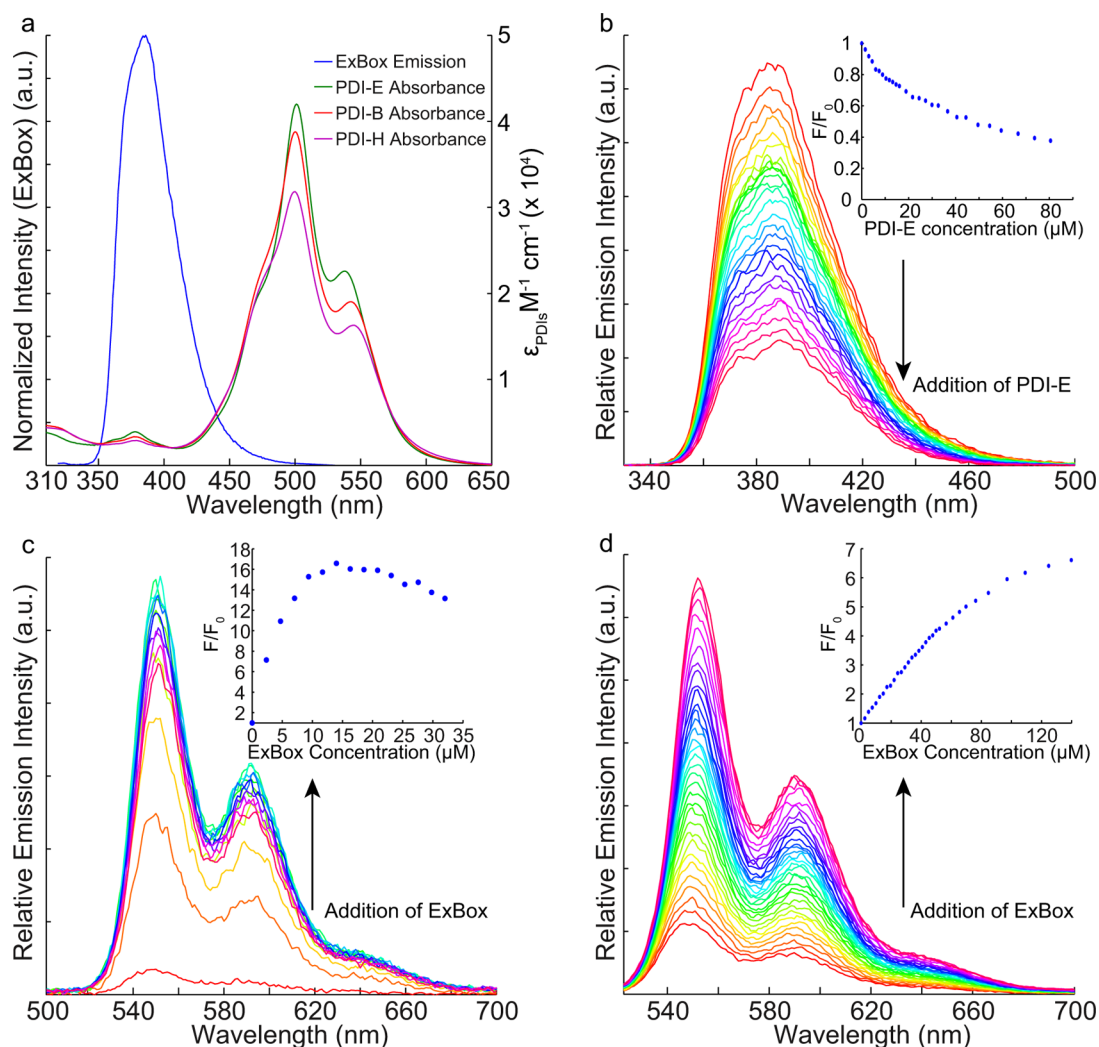


Figure 2. Steady-state photophysical analytical data for PDI-E:ExBox. (a) Overlap of normalized fluorescence emission of ExBox and absorption of PDI-E, PDI-B, and PDI-H. (b) Fluorescence titration of PDI-E into ExBox (H_2O , 10 μM), $\lambda_{\text{ex}} = 319 \text{ nm}$ (inset: normalized fluorescence emission with increasing PDI-E concentration with inner filter effect correction at $\lambda_{\text{mon}} = 384 \text{ nm}$). (c) Fluorescence titration of ExBox into PDI-E (H_2O , 15 μM), $\lambda_{\text{ex}} = 319 \text{ nm}$ (inset: normalized fluorescence emission with increasing ExBox concentration at $\lambda_{\text{mon}} = 550 \text{ nm}$). (d) Fluorescence titration of ExBox into PDI-E (H_2O , 15 μM), $\lambda_{\text{ex}} = 520 \text{ nm}$ (inset: normalized fluorescence emission with increasing ExBox concentration at $\lambda_{\text{mon}} = 550 \text{ nm}$).

S9) for the direct excitation of the PDI chromophore ($\lambda_{\text{ex}} = 520 \text{ nm}$), which can be attributed to the recently documented deaggregating effect of macrocyclic complexation.^{17,19} Expectedly, fluorescence enhancement is larger when the aggregation propensity of the dye is greater, that is, the lower its fluorescence quantum yield in the absence of a host (Table 1).

The fluorescence enhancements were utilized to estimate the binding constants of the host–guest complexes as $1.2 \times 10^5 \text{ M}^{-1}$ for PDI-E, $5.3 \times 10^5 \text{ M}^{-1}$ for PDI-B, and $1.3 \times 10^6 \text{ M}^{-1}$ for PDI-H. This trend is consistent with the expected decrease in electrostatic repulsion between the quaternary ammonium groups of the guest with the tetracationic host as the tether length increases. The approximate binding constants are also consistent with measurements by isothermal titration calorimetry (ITC, Figure S14), which provided binding constants of ca. $5 \times 10^4 \text{ M}^{-1}$, which need to be interpreted as lower limits because the total concentration of PDI (rather than the relevant concentration of monomeric, nonaggregated guest), is being used for data analysis.²⁰

ExBox, similar to its smaller paraquat homologues, acts as a strong electron-acceptor within its host–guest complexes (E_{red}

ca. -0.72 eV),¹¹ which is generally manifested in charge-transfer (CT) bands in their visible absorption spectra.²¹ With the PDI guests, which are themselves electron-deficient (E_{red} ca. -0.70 eV)¹⁷ and act only as weak reducing agents (E_{ox} ca. 1.61 eV),²² no CT bands emerged in the UV/vis titrations of ExBox, an exceptional behavior, which was actually desired for the envisaged applications, including light harvesting and chemosensing. Strikingly, when the PDI chromophore was excited in the resulting host–guest complexes, its fluorescence lifetime increased (to ca. 6.3 ns, determined by time-correlated single photon counting, Table 1 and Figure 3) compared to that of uncomplexed PDIs (ca. 4.5 ns, Table 1 and Figure 3), which suggested a protection of the guest chromophore and ruled out CT induced quenching of the PDI by ExBox. The chromophore protection by ExBox is essentially identical to that exerted by the exceptionally inert macrocyclic host, cucurbit[8]uril (CB[8]).¹⁷ This can be rationalized because quenching by both energy transfer (from PDI* to ExBox) and electron transfer (from PDI* to ExBox, ΔG_{ET} was estimated as $+1.23 \text{ eV}$) would be energetically uphill processes (see Supporting Information).

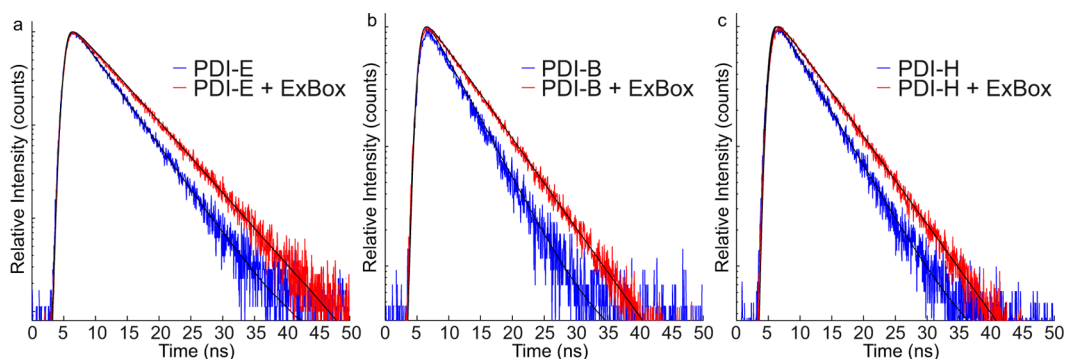


Figure 3. Time-correlated single photon counting decay profiles for (a) **PDI-E** and **PDI-E:ExBox**, (b) **PDI-B** and **PDI-B:ExBox**, and (c) **PDI-H** and **PDI-H:ExBox** ($\lambda_{\text{ex}} = 500$ nm, $\lambda_{\text{mon}} = 550$ nm). All measurements were performed at a guest concentration of $50 \mu\text{M}$. In the cases of the binary complexes, a large excess of ExBox was used.

A number of favorable characteristics of the host–guest system allowed us explore *intermolecular energy transfer* from ExBox (as donor) to PDI (as acceptor) in water. These include (i) the electrochemical properties, which should disfavor photoinduced electron-transfer processes; (ii) the significantly fluorescent nature of ExBox ($\Phi = 0.21 \pm 0.01$, $\lambda_{\text{max}} = 384$ nm, this work), which is in contrast to paraquat homologues; and (iii) the strong absorption of ExBox ($\epsilon_{319\text{nm}} = 69000 \text{ M}^{-1} \text{ cm}^{-1}$), which falls in the spectral window of the PDI chromophore ($\epsilon_{319\text{nm}} = 3400 \text{ M}^{-1} \text{ cm}^{-1}$).

Indeed, the non-negligible overlap (near 450 nm, Figure 2a) between the emission of ExBox and the absorption of the PDIs results in a critical transfer radius of ca. 26.3 \AA (assuming the destacked absorption spectrum of **PDI-E** via complexation with CB[8] is a good approximation for the absorption of PDI inside ExBox and a κ^2 value of $2/3$) such that energy transfer (ET) should kinetically outcompete photoinduced electron transfer. The calculated FRET rates are on the order of 10^{14} s^{-1} assuming a donor–acceptor distance of 3.5 \AA (i.e., a central guest position within the host as found in previously reported X-ray crystal structures), faster than typical photoinduced electron transfer rates for moderately negative or almost thermoneutral ΔG_{ET} values (-1.2 eV or less) (for estimates see Supporting Information).²³ In line with these expectations, the energy transfer efficiency was calculated to be very high (see experiments with polypseudorotaxanes below).

Indeed, although PDI itself shows a residual fluorescence upon excitation at 319 nm, its fluorescence increased dramatically, by factors of 17, 53, and 92 for **PDI-E**, **PDI-B**, and **PDI-H**, when an equimolar amount ($15 \mu\text{M}$) of ExBox (which has its absorption maximum at 319 nm) was added (Figures 2c and S10). Evidently, ExBox serves as an antenna to transfer photonic energy to the PDI dyes, and it does so intermolecularly, through the formation of a host–guest complex. Very likely, the mechanism of ET is Förster resonance energy transfer (FRET), although exchange singlet–singlet energy transfer may also contribute at such short donor–acceptor distances.²⁴ Most importantly, the fluorescence enhancements for a particular PDI dye upon ExBox excitation are much larger (ca. 17–92) than those observed upon their direct excitation (ca. 2.1–12.6, *vide supra*), or that observed for the complex, **PDI-E:CB[8]**, at the excitation wavelength of ExBox (319 nm, factor of 5.5, Figure S11). Consequently, the effects are not simply due to a deaggregating effect of ExBox (in this case, the enhancements should be the same). Instead, they establish a light-harvesting effect of ExBox, an extra increase in

emission by a factor of 7–10, in combination with efficient FRET to the supramolecularly assembled PDI cores, whose fluorescence lifetimes and quantum efficiencies are conserved—actually improved—by the macrocyclic encapsulation. Excitation fluorescence spectra also demonstrate the presence of energy transfer. In the presence of ExBox as host, the emission of **PDI-E** could be efficiently excited in the short-wavelength range of the ExBox absorbance (Figure S12), while in the presence of CB[8] as host, the excitation spectrum corresponded to the absorption of **PDI-E**. To the best of our knowledge, this is the first demonstration of a supramolecular destacking and antenna effect induced through the formation of discrete host–guest complexes in aqueous solution.

Next, we wondered whether our complexes were capable of further hierarchical self-assembly in aqueous media. The complexation of cucurbit[7]uril (CB[7]) with quaternary ammonium motifs in water is established in the literature.²⁵ Therefore, we investigated the complexation of CB[7] with **PDI-B:ExBox** as it has been previously demonstrated that CB[7] is incapable of encapsulating the PDI core,¹⁷ thus presenting two pairs of orthogonal self-assembly motifs.

A ^1H NMR titration of CB[7] into **PDI-B:ExBox** (D_2O , 1 mM) (Figure S15) shows a number of features demonstrating the formation of a 3-polypseudorotaxane (schematically represented in Figure S29): the peaks assigned to the three outer CH_2 groups of the butyl tether, the hydroxyethyl groups and the two methyl groups of the ammonium units all exhibit upfield shifts consistent with complexation with CB[7]; furthermore, the peak assigned to the CH_2 groups next to the imide nitrogens and the PDI aromatic core experiences a downfield shift indicating their proximity to the deshielding carbonyl portals of CB[7]. Peak assignments were performed with the aid of ^1H – ^1H COSY spectra (Figure S16). The complexed ExBox peaks also experience a slight downfield shift. Such behavior demonstrates that CB[7] is in fast exchange with **PDI-B:ExBox** on the NMR time scale. Most interestingly, however, is that upon addition of 0.8 equiv of CB[7], the ratio of complexed to total ExBox increases from 0.6 to 0.8. Addition of two equivalents of CB[7] results in complete disappearance of uncomplexed ExBox peaks, indicating quantitative complexation of the ExBox and **PDI-B** units. Thus, CB[7] aids the deaggregation of **PDI-B** and increases its degree of complexation with ExBox by acting as a dynamic, supramolecular stopper for the **PDI-B:ExBox** complex. Two-dimensional NMR was also carried out to provide further evidence for polypseudorotaxane formation. DOSY NMR of 1:1:2 **PDI-**

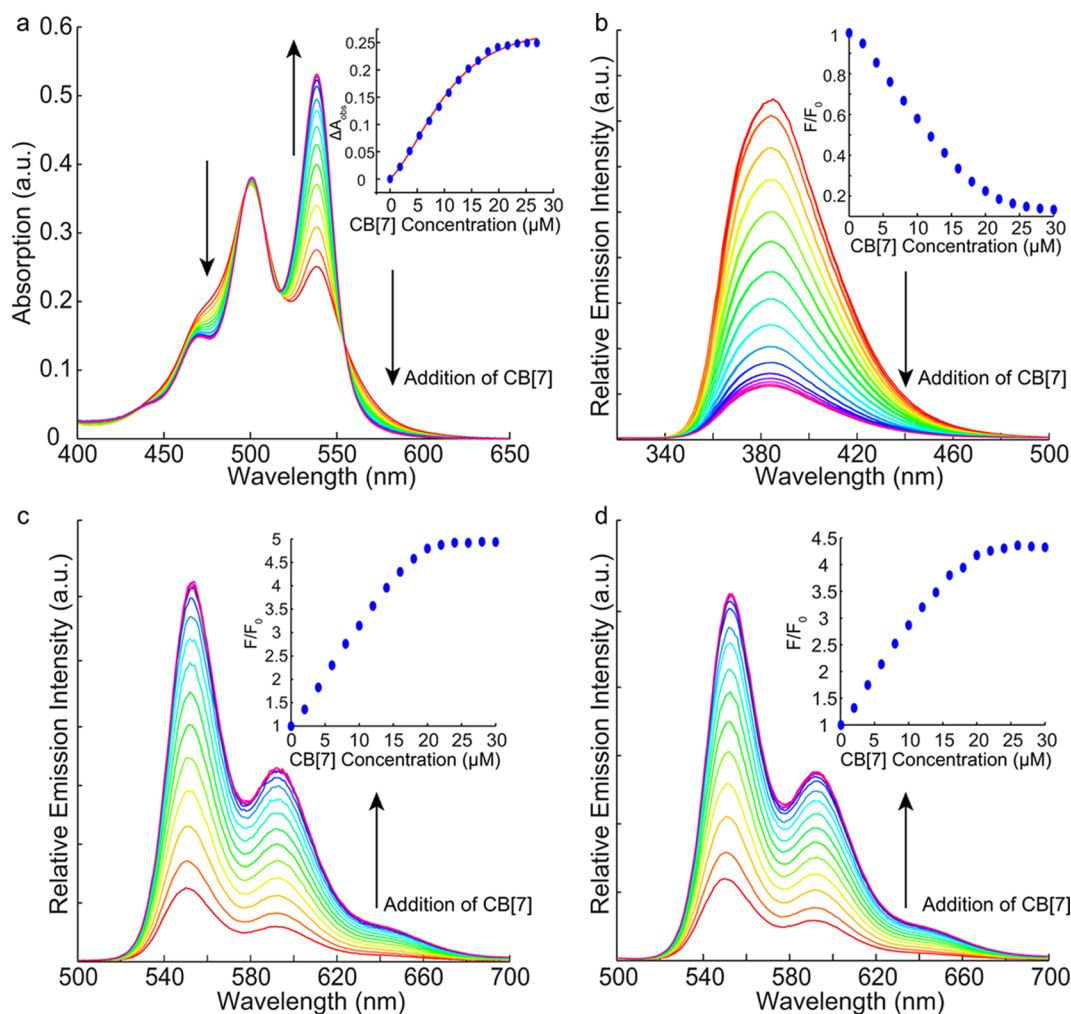


Figure 4. Steady-state photophysical analytical data for **PDI-B:ExBox:CB[7]**. (a) UV/vis titration of **CB[7]** into **PDI-B:ExBox** (H_2O , $10 \mu\text{M}$) (inset: absorption change at 538 nm versus increasing **CB[7]** concentration fitted to a 1:2 binding model giving a combined association constant of approximately 10^{10} M^{-2}). (b) Fluorescence titration of **CB[7]** into **PDI-B:ExBox** (H_2O , $10 \mu\text{M}$), $\lambda_{\text{ex}} = 319 \text{ nm}$ (inset: normalized fluorescence emission with increasing **CB[7]** concentration at $\lambda_{\text{mon}} = 384 \text{ nm}$). (c) Fluorescence titration of **CB[7]** into **PDI-B:ExBox** (H_2O , $10 \mu\text{M}$), $\lambda_{\text{ex}} = 319 \text{ nm}$ and (d) $\lambda_{\text{ex}} = 520 \text{ nm}$ (insets: normalized fluorescence emission with increasing **CB[7]** concentration at $\lambda_{\text{mon}} = 550 \text{ nm}$).

B:ExBox:CB[7] (D_2O , 1 mM) shows that all three components in solution diffuse at equal rates (Figure S17). The spectrum also shows no presence of uncomplexed **ExBox** or **PDI** aggregates. Through-space ROESY NMR (Figure S18) shows correlation between the PDI_{Ar} protons of **PDI-B** and the H_α , H_β and Ph protons of **ExBox** confirming that **ExBox** still encapsulates the **PDI** core in the presence of **CB[7]**. The strength of these correlations was also found to increase upon addition of **CB[7]** relative to the binary complex. A binding stoichiometry for **PDI-B:ExBox:CB[7]** of 1:1:2 was confirmed by the symmetry of the **ExBox** and PDI_{Ar} peaks in the ^1H NMR spectra upon addition of **CB[7]** and by a Job plot, which reveals a maximum at approximately 0.33 (Figure S19). The complicated splitting of the **CB[7]** ^1H NMR peaks, due to an asymmetric binding environment, is also indicative of 1:1:2 binding.²⁶

Having established the formation of the 3-polypseudorotaxane by NMR, we proceeded to investigate the photophysical effects of **CB[7]** on the system. Optical titrations revealed a continued narrowing of UV/vis absorption peaks in the visible region upon addition of **CB[7]**, with an amplified increase in optical density near $520\text{--}550 \text{ nm}$, indicating binding of **CB[7]**

with the ammonium groups and a significant enhancement in the degree of complexation between **ExBox** and **PDI-B** (Figure 4a). An absence of isosbestic points in the absorption titration of **CB[7]** into **PDI-B** in the $400\text{--}700 \text{ nm}$ interval demonstrates that **CB[7]** does not bind to the **PDI** core (Figure S20). The combined effect of **ExBox** and **CB[7]** on the absorption spectrum of **PDI-B** is much greater than the sum of their individual influences (Figure S7). UV/vis titrations were also used to calculate a combined association constant of approximately 10^{10} M^{-2} for 1:2 (**PDI-B:ExBox**):**CB[7]** giving a ternary binding constant in the order of 10^{15} M^{-3} by optical methods.²⁷ TCSPC further confirmed the higher degree of complexation following the addition of two equivalents of **CB[7]** to **PDI-B:ExBox** (1:1), revealing an increase in the excited state lifetime of **PDI-B** to 7.11 ns . Fluorescence titrations of **CB[7]** into **PDI-B:ExBox** (1:1, $10 \mu\text{M}$) and **CB[7]:ExBox** (2:1) into **PDI-B** ($10 \mu\text{M}$) gave average fluorescence enhancements of 30 ± 3 ($\lambda_{\text{ex}} = 520 \text{ nm}$, direct excitation) and 250 ± 10 ($\lambda_{\text{ex}} = 319 \text{ nm}$, indirect excitation) relative to bare **PDI-B** (Figures 4, S21–22). Such an enormous enhancement in **PDI-B** fluorescence output upon excitation of **ExBox**, relative to direct excitation, exemplifies the antenna

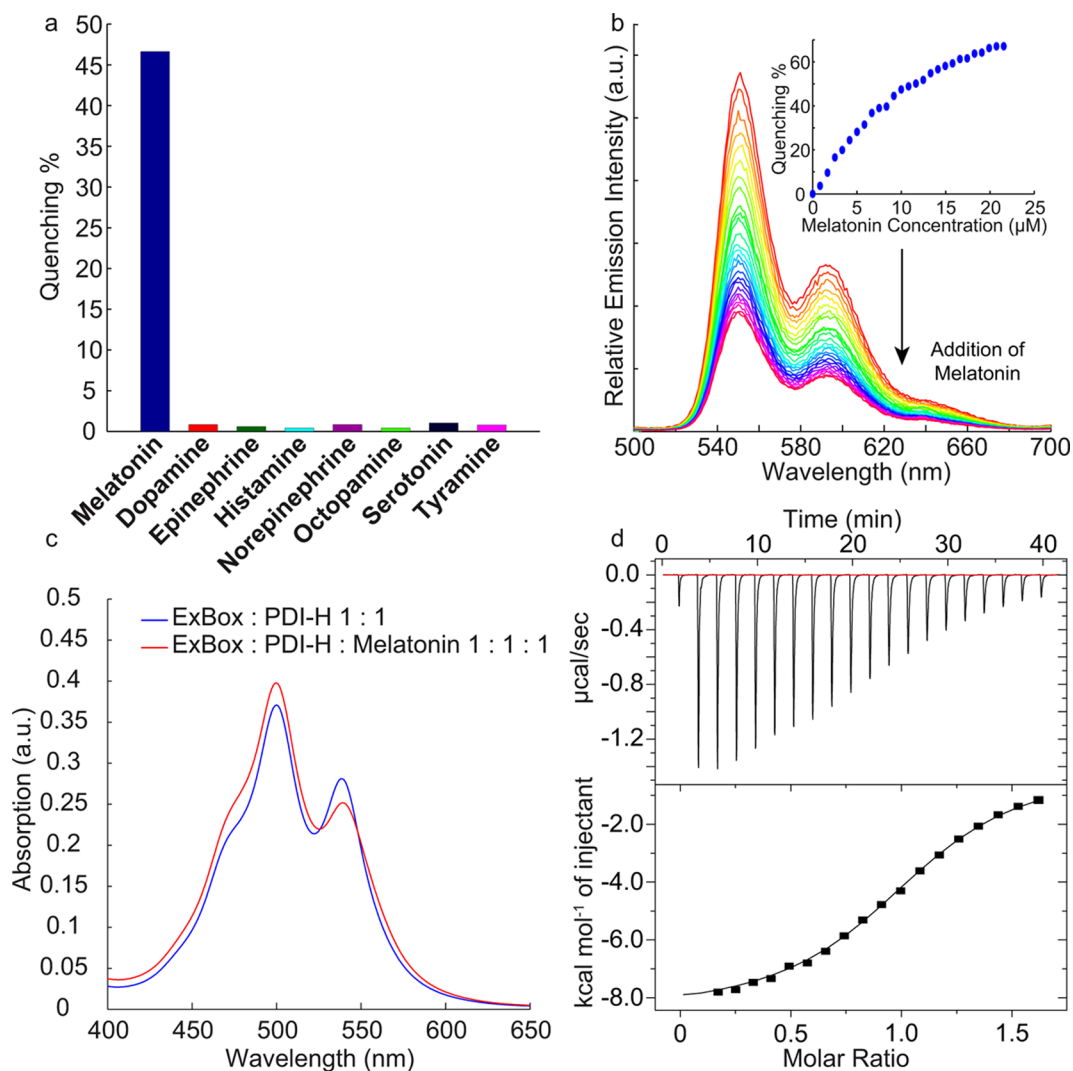


Figure 5. (a) Bar chart showing the percentage quenching of PDI-H fluorescence emission upon addition of 1 equiv of a range of neurotransmitters to 1:1 PDI-H:ExBox (H₂O, 10 μM) $\lambda_{\text{ex}} = 319$ nm, $\lambda_{\text{mon}} = 593$ nm. (b) Fluorescence titration of melatonin into 1:1 PDI-H:ExBox (H₂O, 10 μM), $\lambda_{\text{ex}} = 319$ nm (inset: percentage fluorescence quenching with increasing melatonin concentration, $\lambda_{\text{mon}} = 550$ nm). (c) UV/vis spectra of PDI-H:ExBox 1:1 and PDI-H:ExBox:melatonin 1:1:1 (H₂O, 10 μM). (d) Isothermal titration calorimetry data for melatonin:ExBox ([ExBox] (syringe) = 1 mM, [melatonin] (cell) = 100 μM), giving an association constant (K_a) of $(1.15 \pm 0.07) \times 10^5 \text{ M}^{-1}$.

effect for photonic energy transfer between ExBox and PDI-B. The quantum yield of the stoichiometric ensemble producing the 3-polypseudorotaxane was measured as 0.47 relative to PDI-E. A very small enhancement of PDI-B fluorescence (2.7-fold, $\lambda_{\text{ex}} = 520$ nm and 2.6 fold, $\lambda_{\text{ex}} = 319$ nm) was observed upon addition of two equivalents of CB[7] (Figure S23) confirming that the overall fluorescence enhancement of PDI-B is due to the complexation of both ExBox and CB[7]. The fluorescence of ExBox was also monitored upon addition of CB[7] to PDI-B:ExBox (1:1, 10 μM), which was found to decrease to 11% its original output (Figure 4b). Such an increased quenching of ExBox emission indicates an overall enhancement in the ET efficiency of the ensemble relative to the binary system at stoichiometric ratios due to tighter binding. It was also noted that the incremental increases in total fluorescence output of PDI-B upon addition of CB[7] were larger than the corresponding incremental decreases in total fluorescence output of ExBox (Figure S24). This suggests a concomitant destacking effect contributes to the overall PDI-B

fluorescence alongside energy transfer in the 3-polypseudorotaxane (as well as, presumably, in the binary complexes).

While energy transfer is highly efficient in the polypseudorotaxane structure (up to 90%), the nonvanishing fluorescence of ExBox suggests that energy transfer is nonquantitative. This is a surprising result. A trivial explanation, namely that there is a fluorescent ExBox impurity present in our samples, which is not capable of forming a complex with the PDI dyes, does not receive support from the ¹H NMR characterization, which showed our samples were analytically pure. Conversely, a theoretical explanation, namely that the orthogonality between the transition dipole moments of the extended bipyridinium chromophores in ExBox (aligned along the N–N axis)²⁸ and the acceptor PDI chromophore (also aligned along the N–N axis)²⁹ lowers the orientation factor (κ^2) and therefore the critical transfer radius, appears to be similarly unlikely because it has been shown that energy transfer to PDI chromophores is very efficient even if the orthogonality is strictly enforced through a covalent framework.²⁹ In a noncovalent donor–acceptor complex, the flexibility should easily elevate

orthogonality to sufficiently ensure energy transfer at short donor–acceptor distances. Moreover, crystal structures indicate that the alignment of extended aromatic guests encapsulated inside ExBox is not strictly orthogonal, but tilted (by ca. 45°).¹¹ Finally, since donor and acceptor should be in intimate orbital contact in the host–guest complexes, energy transfer should also be efficient by the Dexter mechanism (vide supra) even if the dipole–dipole mechanism would be “forbidden” by orthogonality. Up to now, we could not exclude any of the above possibilities beyond reasonable doubt with the analytical and spectroscopic equipment, which we have at hand, but with the proof of principle established, namely a highly efficient energy transfer from the host, ExBox, to the guest, PDI, we proceeded to exploit the favorable optical characteristics for a first line of applications.

Indeed, the high on/off fluorescence ratio of **PDI-H** in the presence (on) and absence (off) of ExBox (92 at 1:1 equivalency in 10 μM aqueous solution, $\lambda_{\text{ex}} = 319 \text{ nm}$) should allow for several applications. Here we describe the ability of the **PDI-H:ExBox** complex to act as a fluorescent ET chemosensor via competitive displacement.³⁰ The detection of neurotransmitters is an essential field of research for the diagnosis and treatment of numerous disorders.³¹ Therefore, we screened a range of aromatic-based, small molecule neurotransmitters including dopamine, melatonin and epinephrine for their ability to competitively displace **PDI-H** from the hydrophobic cavity of ExBox. Of all neurotransmitters screened, we found that only melatonin facilitated an appreciable decrease in the fluorescence emission of **PDI-H:ExBox**. While elevated levels of melatonin have recently been linked to increased spontaneous tumor incidence in mice,³² it has also been shown to prevent the death of cultured neuroblastoma cells exposed to amyloid beta, which forms neurotoxic aggregates, demonstrating its potential in the treatment of Alzheimer’s disease.³³ Figures 5 and S25 summarize the interaction between the neurotransmitters and **PDI-H:ExBox**.³⁴

Addition of 1 equiv of melatonin results in a 46% reduction in the fluorescence emission of a 10 μM solution of **PDI-H:ExBox** ($\lambda_{\text{ex}} = 319 \text{ nm}$, $\lambda_{\text{mon}} = 593 \text{ nm}$) due to the formation of a 1:1 melatonin:ExBox charge transfer complex (Figures S26 and S27). However, negligibly small changes in fluorescence emission (<1%, $\lambda_{\text{mon}} = 593 \text{ nm}$) were observed for all other analyzed neurotransmitters including serotonin and L-tryptophan (3% quenching, Figure S28), which have structural similarity to melatonin, demonstrating the selectivity of the system. Indeed, ITC showed that melatonin binds to ExBox in water with an association constant of $(1.15 \pm 0.07) \times 10^5 \text{ M}^{-1}$, which is between the upper and lower limits of binding calculated for **PDI-H:ExBox**. This selectivity to detect melatonin lies in the monocationic nature of all other small-molecule neurotransmitters under neutral as well as physiological pH. The positive charge introduces a Coulombic repulsion between them and tetracationic ExBox. The ability of dicationic **PDI-H** to resist displacement by the monocationic neurotransmitters originates from the powerful hydrophobic effect present in the hexacationic complexes stemming from the PDI core. The ability of melatonin to displace **PDI-H** lies in its neutral character and indole unit which, being larger than the catechol, phenol, and imidazole units of the other neurotransmitters, is better able to fill the ExBox cavity, while not introducing repulsive Coulombic effects.

CONCLUSION

In summary, the self-assembly of a series of highly charged complexes in water composed of tetracationic ExBox and dicationic PDI building blocks has been achieved. The complexes were shown to exhibit energy transfer from ExBox to the PDIs. The use of chromophores as recognition units for the assembly of binary complexes capable of ET represents a novel approach to achieving efficient energy transfer in water, the likes of which is required for photosynthetic biomimetic systems and selective sensory materials for biologically relevant analytes. Such systems also have potential in the development of novel light-harvesting devices. Furthermore, we have demonstrated that our hexacationic complexes are capable of further hierarchical self-assembly using orthogonal recognition motifs to produce a 3-polypseudorotaxane with enhanced photophysical properties. Such assembly also allows for far greater levels of dye deaggregation and ensemble ET efficiency at stoichiometric ratios. Lastly, the **PDI-H:ExBox** complex was also shown to act as a highly selective ET chemosensor for melatonin.

ASSOCIATED CONTENT

Supporting Information

Details of synthesis, experimental methods and additional NMR, UV/vis, fluorescence and ITC data. This material is available free of charge via the Internet at <http://pubs.acs.org>.

AUTHOR INFORMATION

Corresponding Authors

w.nau@jacobs-university
oas23@cam.ac.uk

Notes

The authors declare no competing financial interest.

ACKNOWLEDGMENTS

S.T.J.R. thanks the Cambridge Home and European Scholarship Scheme and the Robert Gardiner memorial scholarship. S.T.J.R., J.D.B., R.J.C., and O.A.S. thank the ERC starting investigator grant ASPIRe (Project No. 240629). J.D.B. thanks Marie Curie IEF (Project No. 273807). I.G., F.B., A.I.L., and W.M.N. thank the Deutsche Forschungsgemeinschaft (DFG, NA-686/5) and the COST Action CM1005 “Supramolecular Chemistry in Water”. The authors also thank Athan Karas for useful discussions and Michael Byrne for his artistic input.

REFERENCES

- (1) (a) Wasielewski, M. R. *Chem. Rev.* **1992**, *92*, 435–461. (b) Lehn, J.-M. *Science* **2002**, *295*, 2400–2403. (c) Li, C.-J.; Chen, L. *Chem. Soc. Rev.* **2006**, *35*, 68–82. (d) Ariga, K.; Kunitake, T. *Supramolecular Chemistry—Fundamentals and Applications*; Springer: Berlin, 2005. (e) Suresh, M.; Mandal, A. K.; Kesharwani, M. K.; Adarsh, N. N.; Ganguly, B.; Kanaparthi, R. K.; Samanta, A.; Das, A. J. *Org. Chem.* **2011**, *76*, 138–144. (f) Gabriel, G. J.; Sorey, S.; Iverson, B. L. *J. Am. Chem. Soc.* **2005**, *127*, 2637–2640.
- (2) Oshovsky, G.; Reinhoudt, D.; Verboom, W. *Angew. Chem., Int. Ed.* **2007**, *46*, 2366–2393.
- (3) (a) Ponnuswamy, N.; Cougnon, F. B. L.; Clough, J. M.; Pantos, G. D.; Sanders, J. K. M. *Science* **2012**, *338*, 783–785. (b) Bradford, V. J.; Iverson, B. L. *J. Am. Chem. Soc.* **2008**, *130*, 1517–1524.
- (4) (a) Pullerits, T. O.; Sundström, V. *Acc. Chem. Res.* **1996**, *29*, 381–389. (b) McDermott, G.; Prince, S.; Freer, A. A.; Hawthornthwaite-Lawless, A. M.; Papiz, M. Z.; Cogdell, R. J.; Isaacs, N. W. *Nature* **1995**, *374*, 517–521. (c) Kühlbrandt, W.; Wang, D. N. *Nature* **1991**, *350*,

- 130–134. (d) Kühlbrandt, W.; Wang, D. N.; Fujiyoshi, Y. *Nature* **1994**, *367*, 614–621. (e) Kühlbrandt, W. *Nature* **1995**, *374*, 497–498. (f) *Primary Processes of Photosynthesis*; Elsevier Scientific Pub. Co.: Amsterdam ; New York, 1977.
- (5) (a) Webber, S. E. *Chem. Rev.* **1990**, *90*, 1469–1482. (b) Watkins, D. M.; Fox, M. A. *J. Am. Chem. Soc.* **1994**, *116*, 6441–6442. (c) Gust, D.; Moore, T. A.; Moore, A. L. *Acc. Chem. Res.* **1993**, *26*, 198–205. (d) Gust, D.; Moore, T. A.; Moore, A. L. *Acc. Chem. Res.* **2001**, *34*, 40–48. (e) Heilemann, M.; Tinnefeld, P.; Sanchez Mosteiro, G.; Garcia Parajo, M.; Van Hulst, N. F.; Sauer, M. *J. Am. Chem. Soc.* **2004**, *126*, 6514–6515. (f) Hausteine, E.; Jahnz, M.; Schwille, P. *ChemPhysChem* **2003**, *4*, 745–748. (g) Hohng, S.; Joo, C.; Ha, T. *Biophys. J.* **2004**, *87*, 1328–1337. (h) Sadhu, K. K.; Chatterjee, S.; Sen, S.; Bharadwaj, P. K. *Dalton Trans.* **2010**, *39*, 4146–4154. (i) Cotlet, M.; Vosch, T.; Habuchi, S.; Weil, T.; Müllen, K.; Hofkens, J.; De Schryver, F. *J. Am. Chem. Soc.* **2005**, *127*, 9760–9768. (j) Neuwahl, F. V. R.; Righini, R.; Adronov, A.; Malenfant, P. R. L.; Fréchet, J. M. J. *J. Phys. Chem. B* **2001**, *105*, 1307–1312.
- (6) Demchenko, A. P. *Introduction to Fluorescence Sensing*; Springer: Berlin, 2009.
- (7) (a) Fehr, M.; Takanao, H.; Ehrhardt, D. W.; Frommer, W. B. *Mol. Cell. Biol.* **2005**, *25*, 11102–11112. (b) Takanao, H.; Chaudhuri, B.; Frommer, W. B. *Biochim. Biophys. Acta* **2008**, *1778*, 1091–1099. (c) Chaudhuri, B.; Hörmann, F.; Lalonde, S.; Brady, S. M.; Orlando, D. A.; Benfey, P.; Frommer, W. B. *Plant J.* **2008**, *56*, 948–962. (d) Deuschle, K.; Chaudhuri, B.; Okumoto, S.; Lager, I.; Lalonde, S.; Frommer, W. B. *Plant Cell* **2006**, *18*, 2314–2325.
- (8) (a) *Conjugated Polyelectrolytes*; Wiley-VCH: Weinheim, 2013. (b) Birch, D.; Rolinski, O. *Res. Chem. Intermed.* **2001**, *27*, 425–446.
- (9) (a) Suresh, M.; Mandal, A. K.; Suresh, E.; Das, A. *Chem. Sci.* **2013**, *4*, 2380–2386. (b) Ishow, E.; Credi, A.; Balzani, V.; Spadola, F.; Mandolini, L. *Chem.—Eur. J.* **1999**, *5*, 984–989. (c) Gallina, M. E.; Baytekin, B.; Schalley, C.; Ceroni, P. *Chem.—Eur. J.* **2012**, *18*, 1528–1535.
- (10) (a) Berberan-Santos, M. N.; Choppinet, P.; Fedorov, A.; Jullien, L.; Valeur, B. *J. Am. Chem. Soc.* **2000**, *122*, 11876–11886. (b) Choppinet, P.; Jullien, L.; Valeur, B. *Chem.—Eur. J.* **1999**, *5*, 3666–3678.
- (11) Barnes, J. C.; Juriček, M.; Strutt, N. L.; Frasconi, M.; Sampath, S.; Giesener, M. A.; McGrier, P. L.; Bruns, C. J.; Stern, C. L.; Sarjeant, A. A.; Stoddart, J. F. *J. Am. Chem. Soc.* **2013**, *135*, 183–192.
- (12) Barnes, J. C.; Fahrenbach, A. C.; Cao, D.; Dyar, S. M.; Frasconi, M.; Giesener, M. A.; Benítez, D.; Tkatchouk, E.; Chernyashvskyy, O.; Shin, W. H.; Li, H.; Sampath, S.; Stern, C. L.; Sarjeant, A. A.; Hartlieb, K. J.; Liu, Z.; Carmieli, R.; Botros, Y. Y.; Choi, J. W.; Slawin, A. M. Z.; Ketterson, J. B.; Wasielewski, M. R.; Goddard, W. A., III; Stoddart, J. F. *Science* **2013**, *339*, 429–433.
- (13) (a) Stoddart, J. F.; Colquhoun, H. M. *Tetrahedron* **2008**, *64*, 8231–8263. (b) Fahrenbach, A. C.; Bruns, C. J.; Cao, D.; Stoddart, J. F. *Acc. Chem. Res.* **2012**, *45*, 1581–1592. (c) Coskun, A.; Spruell, J. M.; Barin, G.; Dichtel, W. R.; Flood, A. H.; Botros, Y. Y.; Stoddart, J. F. *Chem. Soc. Rev.* **2012**, *41*, 4827–4859.
- (14) (a) Juriček, M.; Barnes, J. C.; Dale, E. J.; Liu, W.-G.; Strutt, N. L.; Bruns, C. J.; Vermeulen, N. A.; Ghooray, K. C.; Sarjeant, A. A.; Stern, C. L.; Botros, Y. Y.; Goddard, W. A.; Stoddart, J. F. *J. Am. Chem. Soc.* **2013**, *135*, 12736–12746. (b) Bachrach, S. M. *J. Phys. Chem. A* **2013**, *117*, 8484–8491. (c) Barnes, J. C.; Juriček, M.; Vermeulen, N. A.; Dale, E. J.; Stoddart, J. F. *J. Org. Chem.* **2013**, *78*, 11962–11969. (d) Juriček, M.; Strutt, N. L.; Barnes, J. C.; Butterfield, A. M.; Dale, E. J.; Baldrige, K. K.; Stoddart, J. F.; Siegel, J. S. *Nat. Chem.* **2014**, *6*, 222–228.
- (15) Young, R. M.; Dyar, S. M.; Barnes, J. C.; Juriček, M.; Stoddart, J. F.; Co, D. T.; Wasielewski, M. R. *J. Phys. Chem. A* **2013**, *117*, 12438–12448.
- (16) (a) Würthner, F. *Angew. Chem., Int. Ed.* **2001**, *40*, 1037–1039. (b) Struijk, C. W.; Sieval, A. B.; Dakhorst, J. E. J.; van Dijk, M.; Kimkes, P.; Koehorst, R. B. M.; Donker, H.; Schaafsma, T. J.; Picken, S. J.; van de Craats, A. M.; Warman, J. M.; Zuilhof, H.; Sudhölter, E. J. R. *J. Am. Chem. Soc.* **2000**, *122*, 11057–11066. (c) Li, C.; Wonneberger, H. *Adv. Mater.* **2012**, *24*, 613–636.
- (17) Biedermann, F.; Elmalem, E.; Ghosh, I.; Nau, W. M.; Scherman, O. A. *Angew. Chem., Int. Ed.* **2012**, *51*, 7739–7743.
- (18) (a) Trabolsi, A.; Fahrenbach, A. C.; Dey, S. K.; Share, A. I.; Friedman, D. C.; Basu, S.; Gasa, T. B.; Khashab, N. M.; Saha, S.; Aprahamian, I.; Khatib, H. A.; Flood, A. H.; Stoddart, J. F. *Chem. Commun.* **2010**, *46*, 871–873. (b) Hmadeh, M.; Fahrenbach, A. C.; Basu, S.; Trabolsi, A.; Benítez, D.; Li, H.; Albrecht-Gary, A.-M.; Elhabiri, M.; Stoddart, J. F. *Chem.—Eur. J.* **2011**, *17*, 6076–6087. (c) Li, H.; Zhao, Y.-L.; Fahrenbach, A. C.; Kim, S.-Y.; Paxton, W. F.; Stoddart, J. F. *Org. Biomol. Chem.* **2011**, *9*, 2240–2250.
- (19) Bangping, J.; Dongsheng, G.; Yu, L. *Prog. Chem.* **2013**, *25*, 869–880.
- (20) (a) Guo, D.-S.; Uzunova, V. D.; Su, X.; Liu, Y.; Nau, W. M. *Chem. Sci.* **2011**, *2*, 1722–1734. (b) Dsouza, R. N.; Hennig, A.; Nau, W. M. *Chem.—Eur. J.* **2012**, *18*, 3444–3459.
- (21) *Modern Cyclophane Chemistry*; Wiley-VCH Verlag GmbH & Co. KGaA: Weinheim, 2005; pp 485–518.
- (22) Würthner, F. *Chem. Commun.* **2004**, 1564–1579.
- (23) (a) Marcus, R. A. *Angew. Chem., Int. Ed.* **1993**, *32*, 1111–1121. (b) Hunter, C. A.; Sanders, J. K. M.; Beddard, G. S.; Evans, S. *Chem. Soc., Chem. Commun.* **1989**, 1765–1767. (c) Galoppini, E.; Fox, M. A. *J. Am. Chem. Soc.* **1996**, *118*, 2299–2300. (d) Van Anh, N.; Schlosser, F.; Groeneveld, M. M.; van Stokkum, I. H. M.; Würthner, F.; Williams, R. M. *J. Phys. Chem. C* **2009**, *113*, 18358–18368.
- (24) Scholes, G. D.; Ghiggino, K. P. *J. Phys. Chem.* **1994**, *98*, 4580–4590.
- (25) (a) Wang, Y.; King, J. R.; Wu, P.; Pelzman, D. L.; Beratan, D. N.; Toone, E. J. *J. Am. Chem. Soc.* **2013**, *135*, 6084–6091. (b) Zeng, Y.; Li, Y.; Li, M.; Yang, G.; Li, Y. *J. Am. Chem. Soc.* **2009**, *131*, 9100–9106. (c) Kai, L.; Yao, Y.; Kang, Y.; Liu, Y.; Han, Y.; Wang, Y.; Li, Z.; Zhang, X. *Sci. Rep.* **2013**, *3*, 1–2. (d) Liu, Y.; Fang, R.; Tan, X.; Wang, Z.; Zhang, X. *Chem.—Eur. J.* **2012**, *18*, 15650–15654. (e) Liu, K.; Liu, Y.; Yao, Y.; Yuan, H.; Wang, S.; Wang, Z.; Zhang, X. *Angew. Chem., Int. Ed.* **2013**, *52*, 8285–8289. (f) Yang, H.; Liu, Y.; Yang, L.; Liu, K.; Wang, Z.; Zhang, X. *Chem. Commun.* **2013**, *49*, 3905–3907.
- (26) Freitag, M.; Gundlach, L.; Piotrowiak, P.; Galoppini, E. *J. Am. Chem. Soc.* **2012**, *134*, 3358–3366.
- (27) Thordarson, P. *Chem. Soc. Rev.* **2011**, *40*, 1305–1323.
- (28) Kodaka, M. *J. Am. Chem. Soc.* **1993**, *115*, 3702–3705.
- (29) Langhals, H.; Esterbauer, A. J.; Walter, A.; Riedle, E.; Pugliesi, I. *J. Am. Chem. Soc.* **2010**, *132*, 16777–16782.
- (30) (a) Praetorius, A.; Bailey, D. M.; Schwarzlose, T.; Nau, W. M. *Org. Lett.* **2008**, *10*, 4089–4092. (b) Hennig, A.; Bakirci, H.; Nau, W. M. *Nat. Methods* **2007**, *4*, 629–632.
- (31) Pearl, P.; Hartka, T.; Taylor, J. *Curr. Treat. Options Neurol.* **2006**, *8*, 441–450.
- (32) Anisimov, V. N.; Zavarzina, N. Y.; Zabezhinski, M. A.; Popovich, I. G.; Zimina, O. A.; Shtylick, A. V.; Arutjunyan, A. V.; Oparina, T. I.; Prokopenko, V. M.; Mikhalski, A. I.; Yashin, A. I. *J. Gerontol., Ser. A* **2001**, *56*, B311–B323.
- (33) Pappolla, M. A.; Sos, M.; Omar, R. A.; Bick, R. J.; Hickson-Bick, D. L. M.; Reiter, R. J.; Efthimiopoulos, S.; Robakis, N. K. *J. Neurosci.* **1997**, *17*, 1683–1690.
- (34) In cases where the fluorescence of ExBox is being quenched upon complex formation with a neurotransmitter, ExBox could also be used directly (without PDI) as a chemosensor. The use of the ExBox-PDI complexes as chemosensing ensembles is nevertheless advantageous for two well-defined reasons: (1) The fluorescence enhancement by energy transfer amplifies the signal and increases the sensitivity. (2) The presence of PDI allows for a read-out in the visible region which makes the assay more robust towards background and biological matrix effects as compared to UV detection.